Peer-reviewed version available at Sensors 2019, 19, 2806; doi:10.3390/s19122806

Article

The scientific information model of Chang'e-4 Visible and Near-IR Imaging Spectrometer(VNIS) and in-orbit verification

Chunlai Li [1], Zhendong Wang [1], Rui Xu [1], Gang Lv [1],Liyin Yuan [1],Zhiping He [1,*],Jianyu Wang[1,*]

[1] Key Laboratory of Space Active Opto-Electronics Technology, Shanghai Institute of Technical Physics, Chinese Academy of Sciences; lichunlai@mail.sitp.ac.cn; wangzhendong@mail.sitp.ac.cn; xurui@mail.sitp.ac.cn; lvgang@mail.sitp.ac.cn; yuanliyin@mail.sitp.ac.cn;

* Correspondence: hzping@mail.sitp.ac.cn; Tel: +86 13916614280; jywang@mail.sitp.ac.cn; Tel: +86 13916614280

Received: date; Accepted: date; Published: date

Abstract: The Chang'e-4 (CE-4) lunar rover, equipped with The Visible and Near-IR Imaging Spectrometer(VNIS) which based on acousto-optic tunable filter spectroscopy, was launched to the far side of the moon on December 8, 2018. The detection band of VNIS ranges from 0.45 to 2.4μm. Because of the weak reflection of infrared radiation from the lunar surface, a static electronic phase-locked acquisition method is adopted in the infrared channel for signal amplification. In this paper, full-link simulations and modeling are conducted of the infrared channel information flow of the instrument. The signal/noise characteristics of VNIS are analyzed in depth, and the signal-to-noise(SNR) ratio prediction and laboratory verification are presented. On January 4, 2019, the VNIS started working successfully and acquired high-resolution spectrum data of the far side of the moon for the first time. Through analysis, the SNR ratio is in line with predictions, and the data obtained by VNIS in orbit are consistent with the information model proposed in this paper.

Keywords: The Chang'e-4 lunar rover; Phase-locked; Signal-to-noise ratio; Spectral resolution; Infrared focal plane components;

1. Introduction

The Chang'e-4 (CE-4) lunar rover is the first man-made aircraft launched to the far side of the moon, and its rover (Yutu-2) is equipped with an Visible and Near-IR Imaging Spectrometer(VNIS), which is used to analyze the composition of lunar surface minerals, and inherits form the Chang'E-3 Lunar Rover's Scientific Payloads[1]. The VNIS is a spectrum detector based on AOTF spectroscopy[2], and it has two detection channels - visible near-infrared(VIS/NIR:450~950nm) and short-wave infrared(SWIR:900~2400nm). It performs spectral analysis and imaging detection of minerals on the lunar surface under appropriate solar illumination, and assists in the comprehensive detection of minerals and chemical compositions in the patrol areas. The CE-4 spacecraft was successfully launched on December 8, 2018, and it landed on the moon on January 3, 2019. Then the Visible and Near-IR Imaging Spectrometer (VNIS) powered on and acquired infrared spectrum data of the lunar surface. This paper focuses mainly on simulation analyses and laboratory tests based on the infrared channel design features and information flow model of the instrument, and carries out verification according to the acquired in-orbit data.

2. Instrument description

2.1. Basic principle of The Visible and Near-IR Imaging Spectrometer(VNIS)

The VNIS uses an acousto-optic tunable filter (AOTF) for light splitting. When a beam of multicolor light passes through an optically elastic crystal that vibrates at high frequencies, the monochromatic light of a certain wavelength will be diffracted inside the crystal and transmitted

Preprints (www.preprints.org) | NOT PEER-REVIEWED | Posted: 27 May 2019 doi:10.20944/preprints201905.0314.v1

Peer-reviewed version available at Sensors 2019, 19, 2806; doi:10.3390/s19122806

from it at an angle, and the non-diffracted light travels through the crystal directly in the original direction, thereby achieving the goal of light splitting[3]. The AOTF is a spectroscopic device based on the principle of acousto-optic diffraction, and is composed of a crystal and a transducer bonded on it. The transducer converts the electric signal into ultrasonic vibrations in the crystal, which generate spatially periodic modulations. When an incident light is irradiated to the grating, the wavelength of the diffracted light is related to the frequency of the driving electric signal, and it can be changed by varying the frequency of the electric signal[4].

Table 1. The **characteristics of the Chang'e-4 Visible and Near-IR Imaging Spectrometer(VNIS)**

DESCRIPTION	SPECIFICATION	
	VIS/NIR CHANNEL	SWIR CHANNEL
Spectral range (nm)	450～950	900～2400
Spectral resolution (nm)	2～10	3～12
Field of view (º)	8.5×8.5	ϕ3.58
Number of valid pixels	≥256×256	1
Quantized value (bit)	10	16
S/N ratio (dB)	≥43 (maximum SNR) ≥33 (albedo 0.09, solar elevation angle 45°)	≥46(maximum SNR) ≥31 (albedo 0.09, solar elevation angle 15°)
Detection range (m)	0.7~1.3	
Infrared bands acquisition time	~2 min	

According to this principle, by changing the driving frequency of AOTF crystal through rapid scanning of the time dimension, the wavelength of the diffracted monochromatic light passing through the AOTF changes sequentially, which is functionally equivalent to rapidly switching (in the order of 10μs) the transmission wavelength filter by electronic control. In this way, the spectral information of the target can be obtained by acquiring signals in the time dimension [5]. The VNIS can obtain a spectral image in the VIS/NIR channel and spectral data in the SWIR channel simultaneously. Figure .1 shows the components and basic principle of the VNIS, and Table 1 presents the main Specification of the VNIS. In order to improve the sensitivity of the SWIR channel of the VNIS, a static electronic phase-locked acquisition method is adopted to realize the high sensitivity in the SWIR channel.

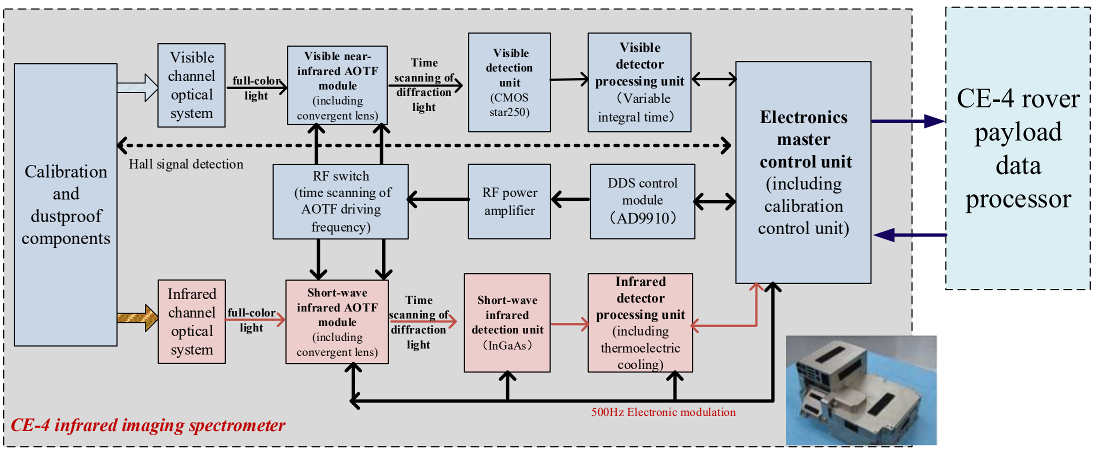

Figure 1. The components and basic principle of the VNIS

2.2. Optical design of the SWIR channel

The optical system of the VNIS in the infrared channel is shown in figure. 2. The target input rays enters into the instrument through an imaging lens and, after being collimated into a parallel beam, drives the AOTF to work, so that the emitted light passing through the AOTF forms an infrared monochromatic light of a specific wavelength and then converges to the detector through a convergent lens.

According to the basic principle of AOTF spectrophotometry, after passing through the AOTF, three lights are formed through the convergent lens, which are +1 level diffraction light, -1 level

Preprints (www.preprints.org) | NOT PEER-REVIEWED | Posted: 27 May 2019 doi:10.20944/preprints201905.0314.v1

Peer-reviewed version available at *Sensors* **2019**, *19*, 2806; doi:10.3390/s19122806

diffraction light and 0 level light[7]. When the system is designed, an InGaAs detector with a diameter of 1mm is placed at the convergence of the +1 level diffraction light, and a light filter is designed for the 0 level light, thereby suppressing the stray light.

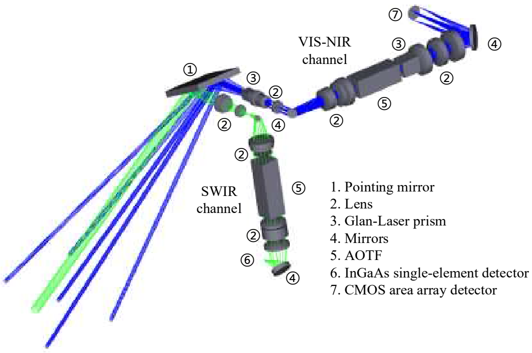

Figure 2. The optical design diagram of the VNIS

2.3. The information link of infrared channel

Figure 3 shows the block diagram of the SWIR channel of the VNIS, which is the basis for building the infrared information flow model. In order to make the AOTF crystal work normal, an radio frequency (RF) signal of a specific frequency should be applied on it, which is generated by the digital display scope (DDS) chip configured with FPGA and then amplified by the RF power amplifier. After the AOTF crystal is driven by the RF signal, the multicolor infrared light entering the AOTF penetrates to produce two channels (+1 level diffraction light and -1 level diffraction light) of monochromatic light and one channel of multicolor 0 level light. In the actual design, we choose to detect the +1 level diffraction light.

Due to the low albedo of the lunar surface, the two channels of infrared monochromatic light after AOTF diffraction are very weak. In order to improve the ability to detect such weak light, a static electronic phase-locked acquisition method is adopted.

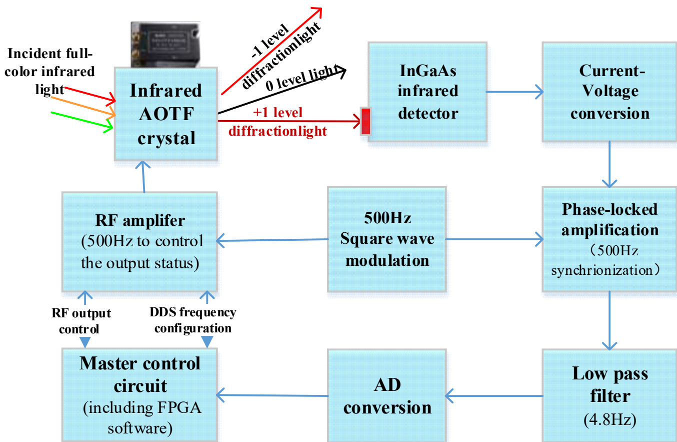

Figure 3. Schematic diagram of the phase-locked processing circuit of infrared channel.

As shown in Figure. 3, by controlling the output RF signal amplified by the power amplifier, the periodic modulation of the output two channels of monochromatic infrared light at the AOTF outlet can be controlled. The modulation frequency is 500 Hz. The +1 level diffraction light after modulation is received by the InGaAs infrared detector, and the corresponding voltage signal is obtained through current-voltage conversion. The signal is processed by a phase-locked amplifier and after low-pass filtering, sent to the AD conversion chip to be converted into a digital signal. It is processed by the FPGA control circuit, which performs on-chip multiple accumulative averaging and then uploads it to the load processor. Figure. 4 shows the picture of the SWIR channel processing circuit and the InGaAs infrared detector.

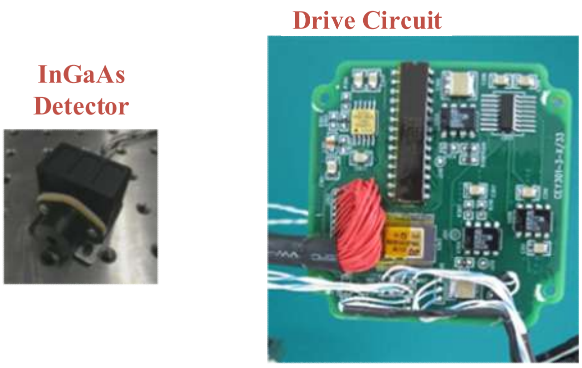

Figure 4. The picture of the SWIR channel processing circuit and the detector. The infrared detector type is J23TE2-66C-R01M-2.6, and is manufactured by Judson, with a peak current response rate of 1.2A/W.

3. Signal flow model simulation and testing

3.1 The signal acquisition model of infrared spectral

The phase-locked amplification method of infrared channel electronics is introduced in section 2.3. In this section, we will further discuss the infrared channel information flow model and signal characteristics. The infrared spectral signal acquisition model is established based on AOTF spectroscopic system, as shown in figure 5.

For weak infrared signal processing technology with phase-locked amplification, moving parts (such as the modulating reticle and chopper) are generally used for modulation between the signal light and background, such as spatial target infrared spectroscopy system [6].In the VNIS, the special point is that a phase-locked amplification model without moving parts is designed according to the characteristics of AOTF, as shown in figure. 5. By controlling the output RF signal amplified by the power amplifier, the model can achieve monochromatic infrared light modulation after AOTF spectrophotometry. The modulation frequency is designed to be 500Hz, which is a purely electronic modulation method, without any moving parts. With the characteristics of great stability and high reliability, it is especially applicable in space.

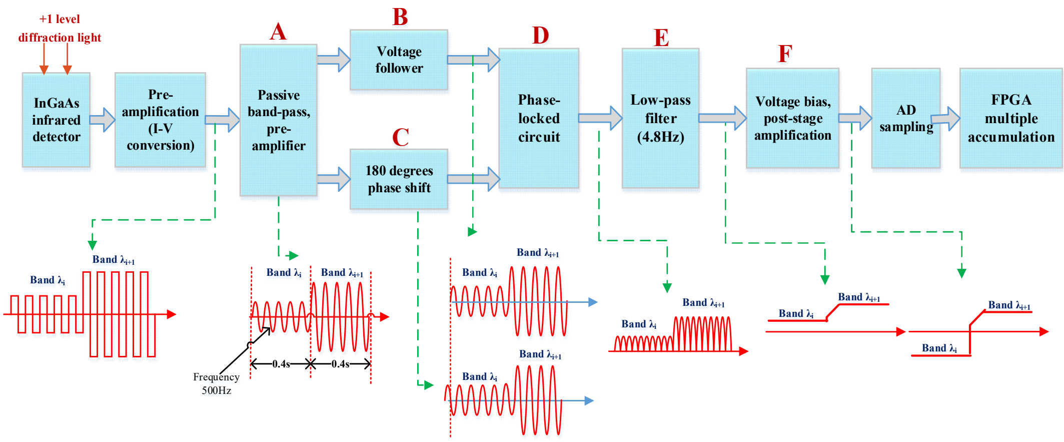

Figure 5. The information flow model of infrared spectrum acquisition based on AOTF modulation

The +1 level diffraction light after passing through the AOTF crystal is received by the InGaAs detector. After current-voltage conversion of a preamplifier, it is sent to the subsequent stage for signal conditioning. As shown in Figure. 5, for two consecutive wavelength signals (band λ_i and band λ_{i+1} in the figure), after 500Hz electronic modulation, what emerges is a periodic (500Hz) infrared analog signal similar to a square wave after passing through the preamplifier. After passive band-

Peer-reviewed version available at Sensors 2019, 19, 2806; doi:10.3390/s19122806

pass and pre-amplification, the square wave appears to be an approximate sinusoidal signal, and the peak of the waveform reflects the intensity of the infrared monochromatic light of the wavelength. Then convert the signal into two signals of the same frequency and the same amplitude but heir phase differs by 180 degrees.

Specifically, one signal is designed as a voltage follower circuit and the other is designed as a reverse circuit, thus realizing a phase shift of 180 degrees. The phase-locked circuit in figure. 5 realizes the chip selection of two signals. It uses a high-speed analog switch (ADG409) to realize phase-locked output so that the signal becomes half the sinusoid shown in the figure. After low pass filtering (4.8Hz), the signal is converted into a corresponding DC level signal, which is fed for AD sampling after voltage bias and post-stage amplification. In order to further improve the detection sensitivity of the system, 8 times of accumulative average processing of single wavelength analog signals are conducted within the FPGA. For infrared full-spectrum detection of lunar surface targets, the time-division detection of different wavelengths is achieved by varying the frequency of the RF signal applied to the AOTF crystal. The VNIS has 300 infrared sampling bands. The acquisition time of a single band is 0.4s, so the acquisition time of the full spectrum channel is approximately 2 minutes.

The above model describes the mechanism of the infrared channel signal generation of the VNIS. At the forefront of the model, the infrared detector produces a photo-generated signal current I(λ) due to receiving infrared light energy P(λ).The model aims to enhance the sensitivity of the infrared channel. Based on the above information flow model, the source of the photo-generated current I(λ) at the input end can be further analyzed so as to obtain the signal-to-noise ratio of the system.

For the lunar surface spectral detection model，the solar radiation is transmitted to the surface of the moon through the space, and the surface of the moon can be approximated as a Lambert body. The target energy P(λ) received by the VNIS can be expressed as[9]：

$$P(\lambda)=\frac{1}{4}\cdot E\cdot D_O{}^2\cdot\Omega\cdot\tau_o\cdot\rho\cdot\sin\theta \qquad (1)$$

where E represents the spectral irradiance of the sun near the lunar surface, D_0 is the optical aperture, Ω is the instantaneous solid angle of observation, τ_0 is the optical system efficiency, θ is the solar elevation angle, $\Delta\lambda$ is the spectral resolution, and ρ is the lunar albedo.

Generally, the target energy P(λ) is determined after the instrument system parameters are determined. That is, given the target radiant power received by the InGaAs infrared detector in the information flow model in figure. 5, the signal current I(λ) of the infrared detector response can be expressed as:

$$I_{s\lambda}=P_\lambda\times A \qquad (2)$$

The VNIS uses the J23TE2-66C-R01M-2.6 infrared detector manufactured by Judson, with a peak current response rate of 1.2A/W. After the signal current of the detector response is determined, the noise current $I_{n\lambda}$ can be calculated by the following equation.

$$I_{n\lambda}=\sqrt{2\times q\times(I_{s\lambda}+I_{dark}+I_{black})\Delta f} \qquad (3)$$

where q represents the electron charge, I_{dark} denotes the dark current of the detector, I_{black} denotes the current caused by the thermal background radiation, and Δf is the bandwidth of the information processing circuit. Due to the rapid development of the detector technology, the dark current of the InGaAs infrared detector at a low temperature of around -40°C is basically zero. The SNR can be simplified as：

$$\mathrm{SNR}(\lambda)=\frac{I_{s\lambda}}{I_{n\lambda}}=\frac{I_{s\lambda}}{\sqrt{2\times q\times I_{s\lambda}\Delta f}}=\sqrt{\frac{I_{s\lambda}}{2\times q}}\frac{1}{\sqrt{\Delta f}} \qquad (4)$$

As can be seen, given the system design parameters and the selected infrared detector, the system SNR is directly related to the information processing bandwidth Δf of the circuit. The system

Peer-reviewed version available at *Sensors* **2019**, *19*, 2806; doi:10.3390/s19122806

adopts the information flow model shown in figure 5. Here, Δf is actually the low-pass filtering 4.8Hz mentioned in the figure.5, and the system noise beyond ((500-2.4)Hz~(500+2.4)Hz) is filtered out.

In contrast, if the direct signal acquisition method (without phase lock-in method) is adopted, the bandwidth Δf is generally around 2000Hz, which is the mechanism of increasing the SNR ratio. The figure. 6 shows the estimated SNR curve based on the static electronic phase-locked acquisition method (bandwidth is about 4.8Hz), which is compared with the direct signal acquisition method (bandwidth is about 2000Hz).

As shown in figure. 6, there exists a step at 1.4μm. The reason is that the AOTF crystal has two channels, and the 1.4μm is exactly the switching point of the two channels. The input conditions for the above evaluation are a lunar albedo of 0.09 and a solar elevation angle of 15 degrees. It can be seen from the figure 6 that the SNR is about 600 in the 1.7μm.

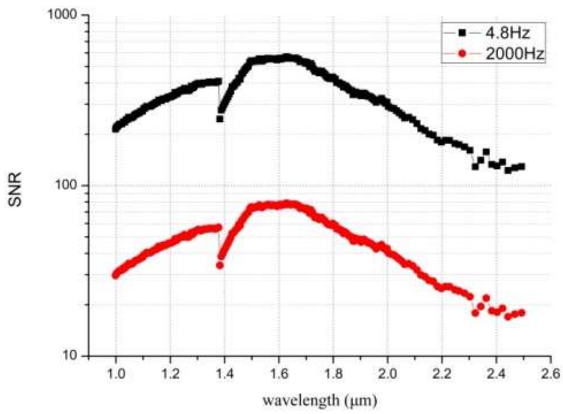

Figure 6. The Signal-to-noise ratio（SNR） curve comparison between the static electronic phase-locked acquisition method(black) and the direct signal acquisition method(red).

3.2 Laboratory testing and evaluation

After the information flow model is established and the system signal-to-noise ratio is analyzed, the signal characteristics and signal-to-noise ratio of the instrument are tested in the laboratory. Shown in Fig. 7 is a photo of laboratory testing, where the light source is a searchlight and the target is 90% reflectivity calibration plate. Fig. 8 shows the original digital number (DN)values of 300 infrared spectral bands, and the signal-to-noise ratio at 1.7μm is about 500(the signal DN is 1600, and the noise DN is about 3.2). This is slightly different from the value (600) given in Section 3.1, because the light source here is not the sunlight with an equivalent elevation angle of 15 degrees and its target albedo is not 0.09. In order to further validate the information flow model, the analog signal of the 1.7μm spectrum of the infrared signal in the whole spectrum acquisition process of the system is measured by an oscilloscope. Figure. 9 shows the signal waveforms of A, B, C and D in the model in figure 5, and the characteristics of the waveforms are consistent with the predictions of the established information flow model.

Preprints (www.preprints.org) | NOT PEER-REVIEWED | Posted: 27 May 2019 doi:10.20944/preprints201905.0314.v1

Peer-reviewed version available at *Sensors* **2019**, *19*, 2806; doi:10.3390/s19122806

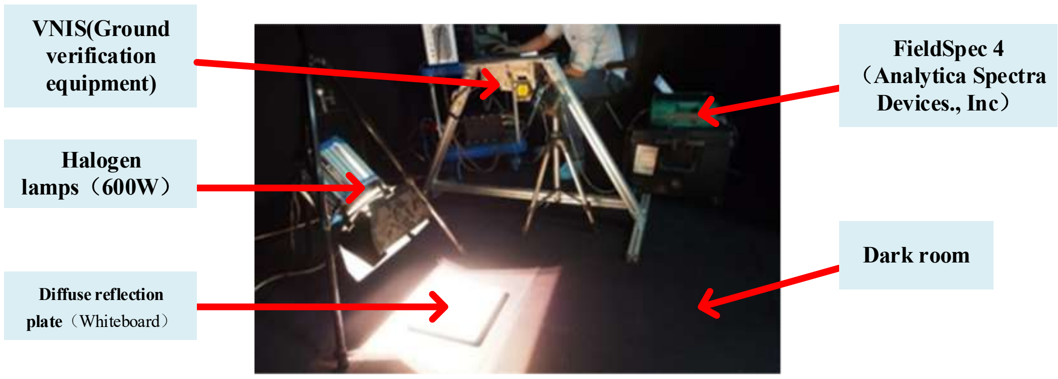

Figure 7. The experimental test was carried out in a dark room, using halogen lamps (600W) to illuminate the diffuse reflective whiteboard (reflectance ＞90%), and then at the same angle, using both VNIS (ground verification equipment) and ground spectrometer (FieldSpec 4, Analytica Spectra Devices) ., Inc) measures the diffuse reflectance spectrum[10].

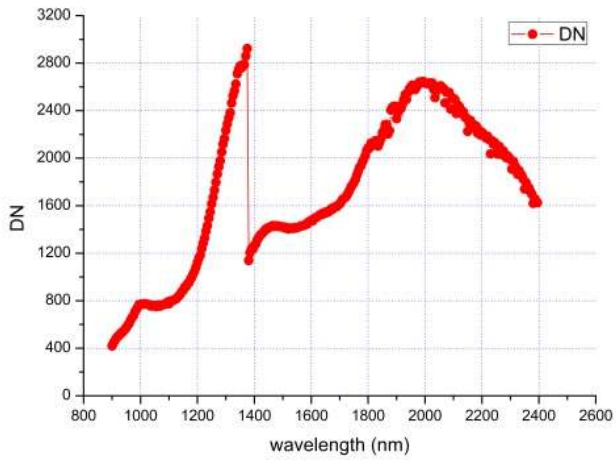

Figure 8. The original infrared full spectrum signal measured in the laboratory.

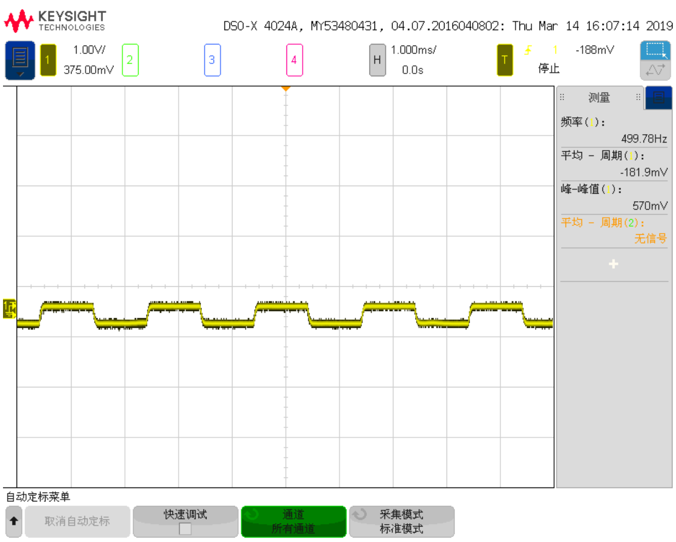

(a) The analog displayed by oscilloscope of infrared signal after I-V conversion (The point A in figure 5.)

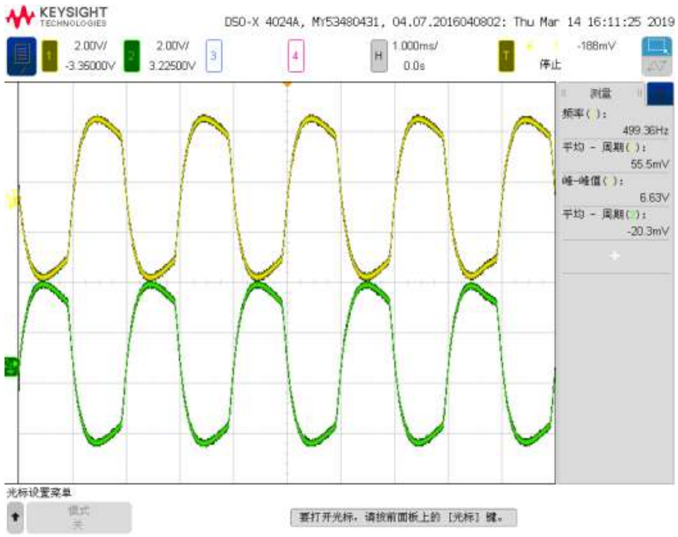

(b) The analog displayed by oscilloscope of the infrared signals before phase-locked circuit (The yellow is for point B in figure 5, and the green is for point C in figure 5)

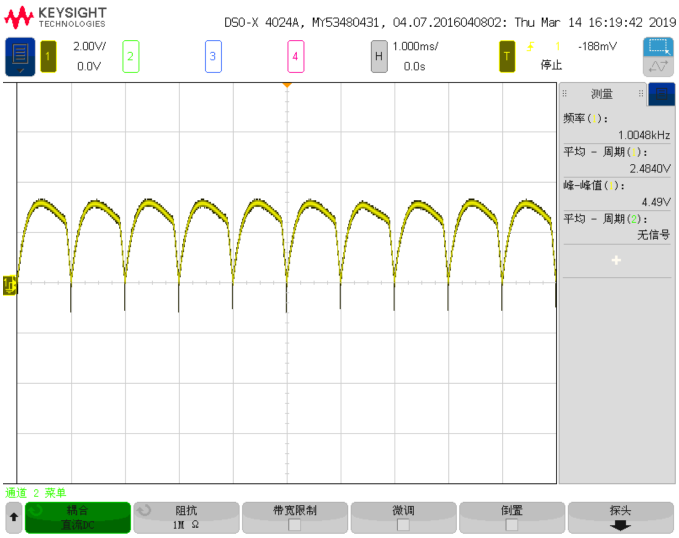

(c) The analog displayed by oscilloscope of the infrared signal after phase-locked circuit (The point D in figure 5.)

Figure 9. The signals of VNIS at band 1.7μm displayed by the oscilloscope(corresponding to A, B, C and D in figure. 5)

4. In-orbit testing

On January 4, 2019, the instrument obtained the infrared spectrum data of the first scene on the far side of the moon.Figure.10 shows the scene of the first infrared spectrum on the far side of the moon. The DN values of the original infrared spectrum data of A Point and its full-spectrum SNR are show in figure 11 and figure 12, and the figure 13 gives the infrared spectral reflectance curve of the moon surface at A point[8]. In the test, the solar elevation angle is about 15 degrees and the lunar albedo is about 9%. According to the obtained raw data, the signal-to-noise ratio at 1.7μm is calculated to be around 470, which is basically consistent with the prediction in Section 3.1(Fig.6). This test validates the proposed AOTF system infrared spectral information processing model based on phase-locked amplification technology and also verifies the high sensitivity of the lunar surface weak infrared signal detector.

doi:10.20944/preprints201905.0314.v1

Peer-reviewed version available at *Sensors* **2019**, *19*, 2806; doi:10.3390/s19122806

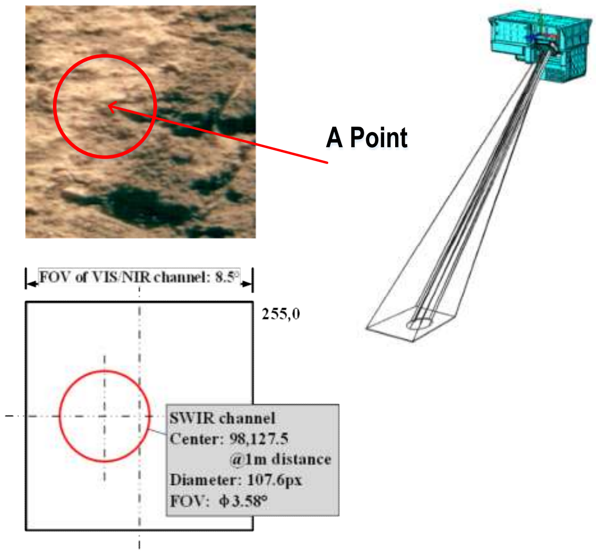

Figure 10. The first scene(which is defined as A point) obtained by VNIS on the far side of the moon. The VNIS is used to detect lunar surface objects and the optical axis of the VIS/NIR channel and SWIR channel is paralleled each other at an 18 mm distance [10, 11]. The FOVs in the VIS/NIR and SWIR are 8.5° × 8.5° and Φ3.58°, respectively. The circle represents the SWIR channel's FOV, which has a diameter of 107.6 pixels and is centered at the coordinate (98, 127.5) of the VIS/NIR image in 1m detection distance typically.

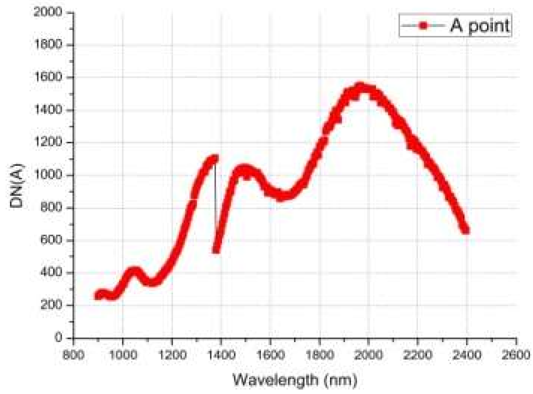

Figure 11. The original DN values of the far side of the moon surface at the A point.

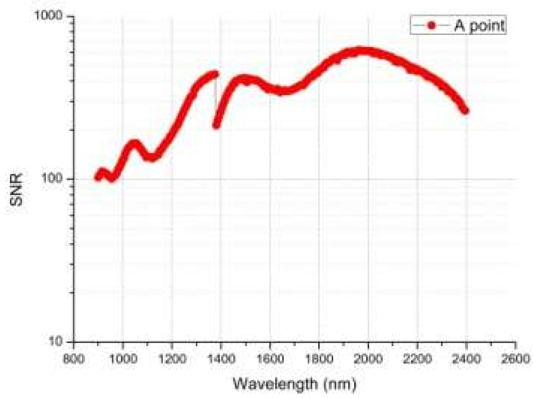

Figure 12. The full-spectrum SNR curve of the far side of the moon surface at the A point.

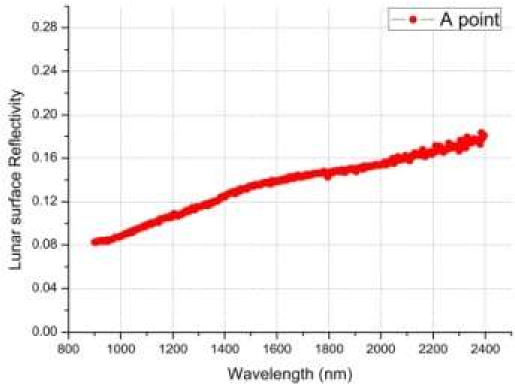

Figure 13. The spectral reflectance curve of the far side of the moon surface at the A point.

5. Conclusions

In view of the extremely weak infrared reflectance spectral signals on the lunar surface, a method of a static electronic phase-locked acquisition in infrared channel is proposed. In addition, the paper establishes an information flow model, on the basis of which the signal-to-noise ratio has been predicted. As of the end of February 2019, the VNIS has operated 6 times on the lunar surface, and acquired 12 sets of infrared spectral data. It is found that an average SNR of 300 can still be obtained when the lunar albedo is around 9% and the solar elevation angle is 15 degrees, which further verifies the effectiveness of the proposed static electronic phase-locked acquisition method for weak infrared targets. The SNR values of in-orbit testing are basically consistent with the predictions given in this paper. In China's future deep space exploration programs, the method proposed in this paper will be helpful to further study the acquisition of weak infrared spectral information on the surface of planets.

Acknowledgments: This paper was supported by the Chinese lunar exploration program's special funds for the second phase and the National Natural Science Foundation (No. 21105109, No. 61605231). The authors thank the Science and Application Center for Moon and Deep Space Exploration of the Chinese Academy of Sciences for the ground test and data preprocessing, and the National Space Science Center of the Chinese Academy of Sciences for its contributions to the development and testing of the instruments.

References

1. S. W. , Dai, J., Wu, H. X., Sun, B. M., Zhang, J. F., Yang, G. Y., Fang, J. Y., Wang, H. Y., Wang, andJ. S., An (**2014**). Chang'E-3 Lunar Rover's Scientific Payloads. Chinese Journal of Space Science, 34(3), 332-340.
2. O. Korablev, J.-L. Bertaux, A. Grigoriev, E. Dimarellis, Yu. Kalinnikov, A. Rodin, C. Muller and D. Fonteyn. An AOTF-based spectrometer for the studies of Mars atmosphere for Mars Express ESA mission. Adv. Space Res. 29:2 pp. 143-150, **2002**
3. Z.P, He, B.Y., Wang, G., Lv, C.L., Li, L.Y., Yuan, R., Xu, K., Chen, and J. Y.,Wang, "Visible and Near-Infrared Imaging Spectrometer (VNIS) and Its Preliminary Results from the Chang'E 3 Project",Rev. Sci. Instrum., 86,8 (**2014**).
4. Z.P., He, B.Y.,Wang, G., Lv, C.L., Li, L.,Y.,Yuan, R., Xu, B.,Liu, K.,Chen and J.Y.,Wang, "Operating principles and detection characteristics of Visible and Near-Infrared Imaging Spectrometer (VNIS) in Chang'e 3", Res. Astron. Astrophys. 14(12), 1567 (**2014**).
5. J. Wang, Z. He, R. Shu, R. Xu, K. Chen, and C Li, "Visible and Near-infrared Imaging Spectrometer aboard Chinese Chang'E-3 Spacecraft", Ch. 5 in Optical Payloads for Space Missions, S-E Qian, Ed., ISBN:9781118945148, John Wiley & Sons (**2015**)
6. Liyin YUAN, Zhiping HE, Gang LV, Yueming WANG, Chunlai LI, Jia'nan XIE, AND Jianyu WANG: Optical design, laboratory test, and calibration of airborne long wave infrared imaging Spectrometer, OPTICS EXPRESS, **2017**,25(19),pp22440-22454.

7. Z.P., He, B.Y.,Wang, G.,Lv, C.L., Li, L.,Y., Yuan, R., Xu, B.,Liu, K.,Chen and J.Y.,Wang, "Visible and Near-infrared Imaging Spectrometer (VNIS) for Chang'E-3", Proc. SPIE 9263, 92630D-1 (**2014**).
8. B.,Liu, J.,Liu, G.,Zhang, Z.,Ling, J., Zhang, Z.,He, B.,Yang, and Y.,Zou, "Reflectance conversion methods for the VIS/NIR imaging spectrometer aboard the Chang'E-3 lunar rover: based on ground validation experiment data," Res. Astron. Astrophys. 13(7), 862 (**2013**).
9. J. Y.,Wang, R., Shu, Y. N.,Liu, and Y. H.,Ma (**2011**). Introduction of Imaging spectral technology. Beijing: Science Press.
10. R., Xu, Z. P.,He, H.,Zhang, Y. H.,Ma, Z. Q.,Fu, and J. Y.,Wang, (**2012**). Calibration of imaging spectrometer based on acousto-optic tunable filter (AOTF). In SPIE Asia-Pacific Remote Sensing, pp. 85270S-85270S, International Society for Optics and Photonics.
11. Z.,He, B., Wang, G.,Lv, C.,Li, L.,Yuan, R., Xu, K.,Chen, and J.,Wang, "Visible and Near-infrared Imaging Spectrometer (VNIS) For In-situ Lunar Surface Measurement", Proc. SPIE 9639, 96391S(**2015**).